Department of Mechanical Engineering

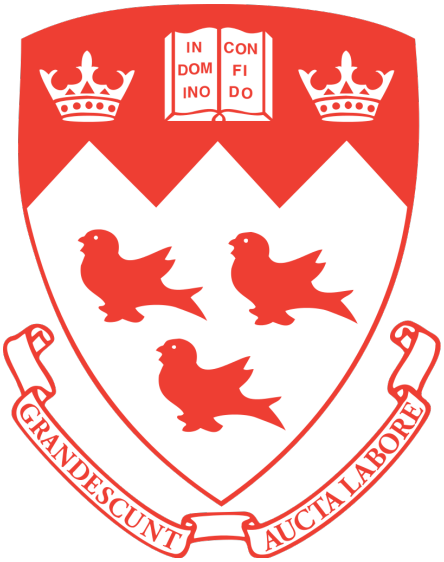

MECH309: Numerical Methods

Final Project Report

Murman-Cole Scheme for the Transonic Small Disturbance Equation

Zhuohua Qiao, 260779462

Jason Zhou, 260663823

Jichuan Yu, 260932708

December 4, 2019

Table of Contents

List of Figures

Introduction

In this project, we attempt to solve the transonic small disturbance (TSD) theory over a circular arc airfoil at various Mach numbers using the Murman-Cole method [1]. The procedure described in [2] is carefully followed in deriving the necessary equations and writing our MATLAB script. The solutions are then visualized and analyzed, with particular focus on shock formation on the airfoil.

The simplified TSD equation for the perturbation potential, given as

$$[(1 - M_\infty^2) - (\gamma + 1)M_\infty^2 \frac{\phi_x}{U_\infty}]\phi_{xx} + \phi_{yy} = 0 \tag{1}$$

is a non-linear partial differential equation. For the purpose of this project, we use the following values for the constants: the specific heat ratio for air $\gamma = 1.4$, the gas constant $R = 287.058 Jkg^{-1}K^{-1}$, the freestream static temperature, $T_\infty = 293K$, and pressures $P_1 = 100kN/m2$. The freestream Mach number M_∞ is an independent variable. The freestream velocity U_∞ is thus a function of M_∞, and can then be calculated using isentropic relation:

$$U_\infty = M_\infty \sqrt{\gamma R T_\infty} \tag{2}$$

Converted to a system of linear equations, Equation 1 can be solved using iterative methods, such as Gauss-Seidel, in the domain around a circular arc airfoil to study the air flow behavior. The impacts of the freestream Mach number as well as the grid size are discussed based on the observation of the pressure coefficient plots along the airfoil surface as well as the pressure contours. The efficiency and accuracy of the numerical method are also studied.

Discussion of Method

To apply numerical methods to solve the TSD equation, the interested domain is first discretized into computational grids as shown in Figure 1.The leading edge of airfoil is located at x = 20 and trailing edge is located at x = 21.

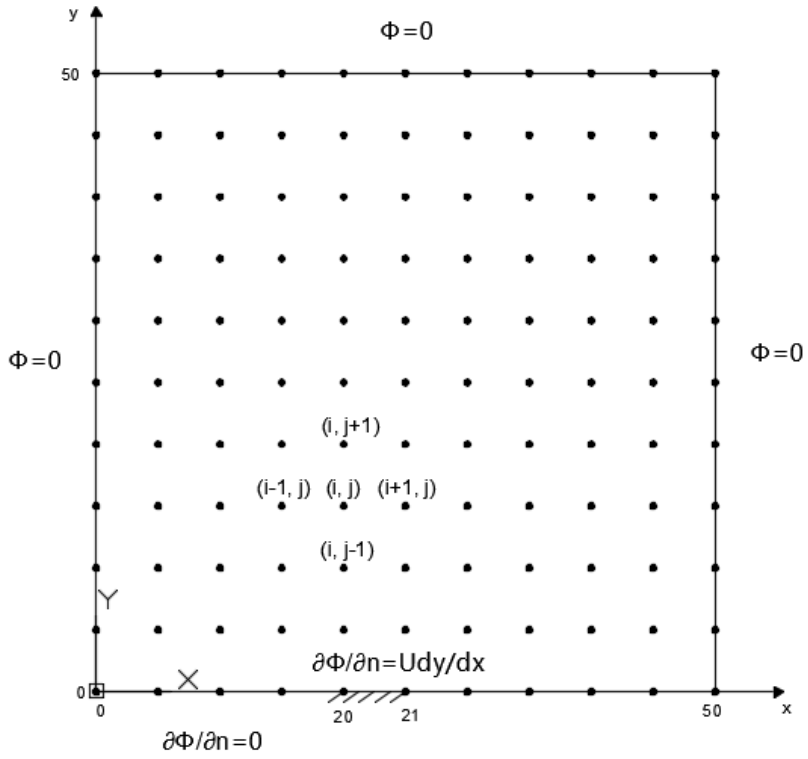

Figure 1: Discretized domain with stencils and boundary conditions.

Using finite-difference formulas for the first order derivative ϕ_x as well as the second order derivatives ϕ_{xx} and ϕ_{yy} on each grid point, the Murman-Cole equation can be written as [1]

$$\begin{aligned}&\frac{(1-\mu_{i,j}A_{i,j})}{(\Delta x)^2}\phi_{i+1,j}+[\frac{\mu_{i-1,j}A_{i-1,j}}{(\Delta x)^2}-\frac{2(1-\mu_{i,j})A_{i,j}}{(\Delta x)^2}-\frac{2}{(\Delta y)^2}]\phi_{i,j}+\frac{1}{(\Delta y)^2}\phi_{i,j+1}\\&+[\frac{(1-\mu_{i,j}A_{i,j})}{(\Delta x)^2}-\frac{2\mu_{i-1,j}A_{i-1,j}}{(\Delta x)^2}]\phi_{i-1,j}+\frac{\mu_{i-1,j}A_{i-1,j}}{(\Delta x)^2}\phi_{i-2,j}+\frac{1}{(\Delta y)^2}\phi_{i,j-1}=0\end{aligned} \tag{3}$$

where, using centered difference for ϕ_x

$$A_{i,j} = (1 - M_\infty^2) - (\gamma + 1)\frac{M_\infty^2}{U_\infty}\frac{\phi_{i+1,j} - \phi_{i-1,j}}{2\Delta x} \tag{4}$$

and

$$\mu_{i,j} = \begin{cases} 0 & \text{if } A_{i,j} > 0 \\ 1 & \text{if } A_{i,j} < 0 \end{cases}$$

Using these equations on each point within the domain D except on the boundary (including the second row from the left due to the $\phi_{i-2,j}$ term), we can obtain a system of linear equations about

$$\boldsymbol{\phi} = \{\phi_{i,j}\} \quad \forall \quad (i,j) in D \tag{5}$$

Gauss-Seidel is used in this project to solve this system of linear equations. Equation 3 is in the form of:

$$a_{i,j}\phi_{i+1,j} + b_{i,j}\phi_{i,j} + c_{i,j}\phi_{i,j+1} + d_{i,j}\phi_{i-1,j} + e_{i,j}\phi_{i-2,j} + f_{i,j}\phi_{i,j-1} = 0 \tag{6}$$

where $a_{i,j}$, $b_{i,j}$, ... are constant coefficients specific to each point in the domain in each iteration. Hence, the element wise form to solve for $\phi_{i,j}$ in each iteration becomes:

$$\phi_{i,j} = \frac{-1}{b_{i,j}}[a_{i,j}\phi_{i+1,j} + c_{i,j}\phi_{i,j+1} + d_{i,j}\phi_{i-1,j} + e_{i,j}\phi_{i-2,j} + f_{i,j}\phi_{i,j-1}] \tag{7}$$

The coefficients are updated by the latest values of $\phi_{i,j}$ before updating the value of $\phi_{i,j}$ in each iteration. All values of $\phi_{i,j}$ are initialized to 0. The boundary conditions are shown in Figure 1, where the airfoil ($20 \leq x \leq 21$) is simulated with a function:

$$y(x) = (\frac{t}{c})(-2x^2 + 82x - 840) \quad \forall (x,0) \in 20 \leq x \leq 21 \tag{8}$$

A coarse grid ($\Delta x = \Delta y = 0.1$), a medium grid ($\Delta x = \Delta y = 0.05$) and a fine grid ($\Delta x = \Delta y = 0.025$) are applied. See the following sections for result discussions.

Question 2

The results of solving the TSD equation with a coarse grid at various Mach numbers are visualized in convergence plots, surface pressure plots and pressure contours, as illustrated on the following pages in Figure 2, 3 and 4.

Figure 2 shows the convergence of the Gauss-Seidel algorithm. Generally, it takes iterations in the order of 10^4 to reach a residual less than 10^{-4} for coarse grid. Higher Mach number turns to take relatively more iterations to converge, which can be explained by the sharper peak and shock of the pressure coefficient plot.

Figure 3 shows the pressure coefficient along the airfoil for different Mach numbers. Negative c_p is chosen to be the vertical axis. The pressure coefficient c_p is a normalized parameter indicating the relative pressure distribution throughout a flow field. when the air flow passes by, because of the existence of the prominent arc airfoil, the negative pressure coefficient in the front of the airfoil is less than zero, while it rises up to a peak and goes down significantly along the airfoil. While we increase the Mach number, the peak becomes sharper, and a shock appears on the right side at a Mach number larger than 0.83. Because of the coarse grid, the pressure coefficient plot is not smooth and hence the shock is not able to be shown clearly. We can observe the shock with the help of the pressure contour plots.

Figure 4 shows the pressure contours for different Mach numbers. It appears that there are 3 extreme points in the domain $[19.5, 21.5] \cup [0, 1]$. A shock appears vertically in the domain when the Mach number is at 0.83 or 0.85.

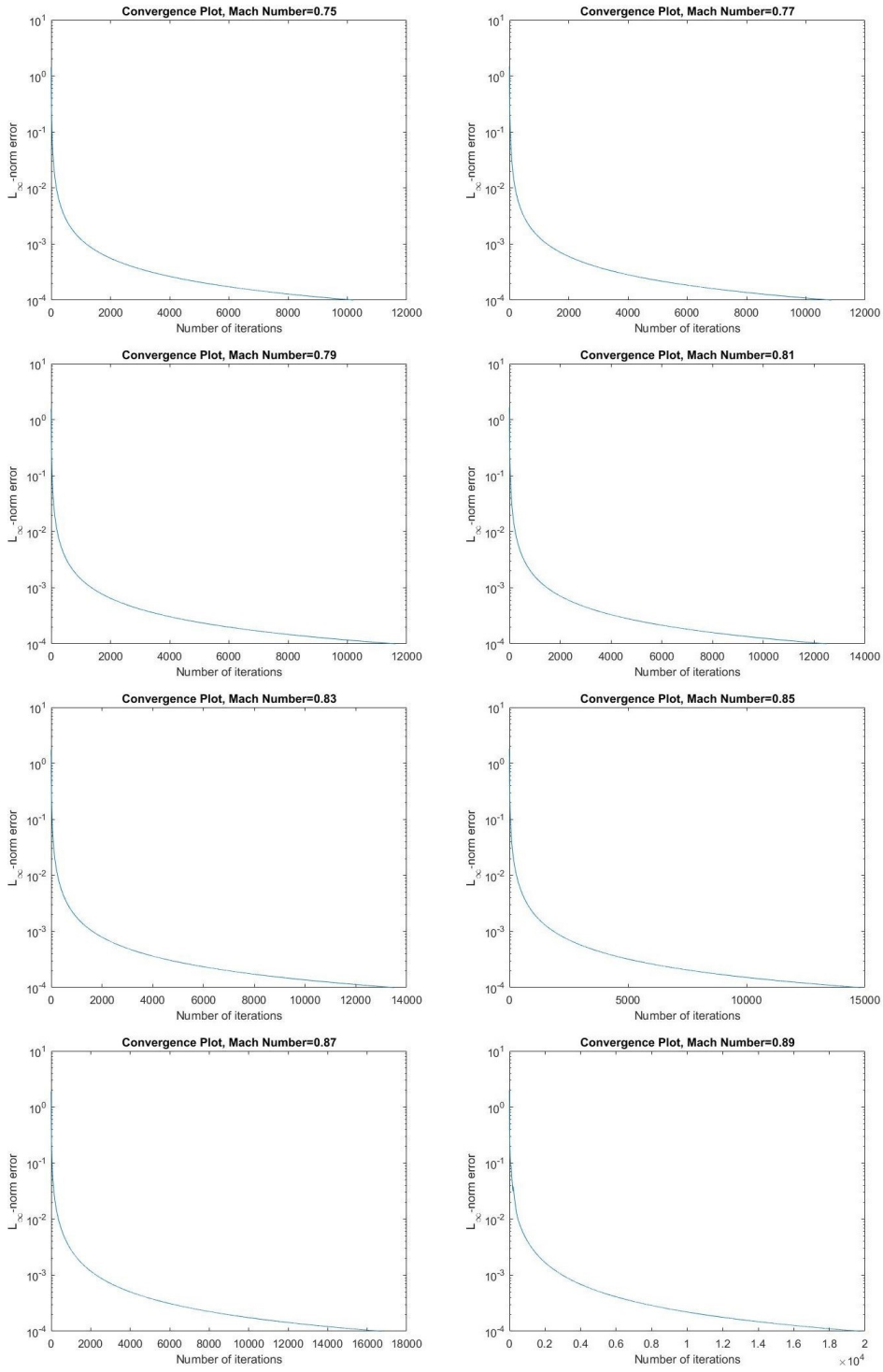

Figure 2: Convergence plots, coarse grid, various Mach Numbers.

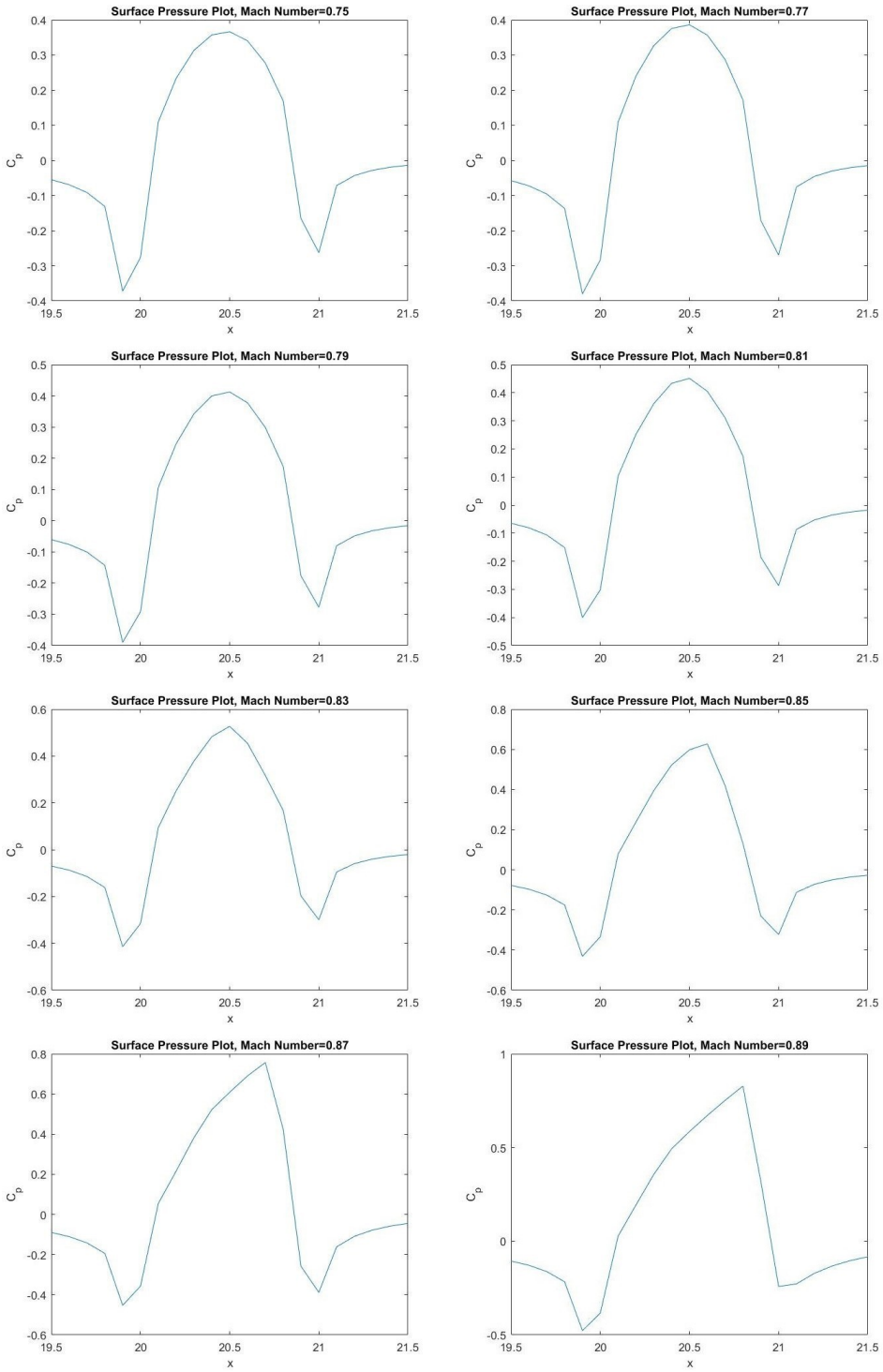

Figure 3: Surface pressure (c_p) plots, coarse grid, various Mach Numbers.

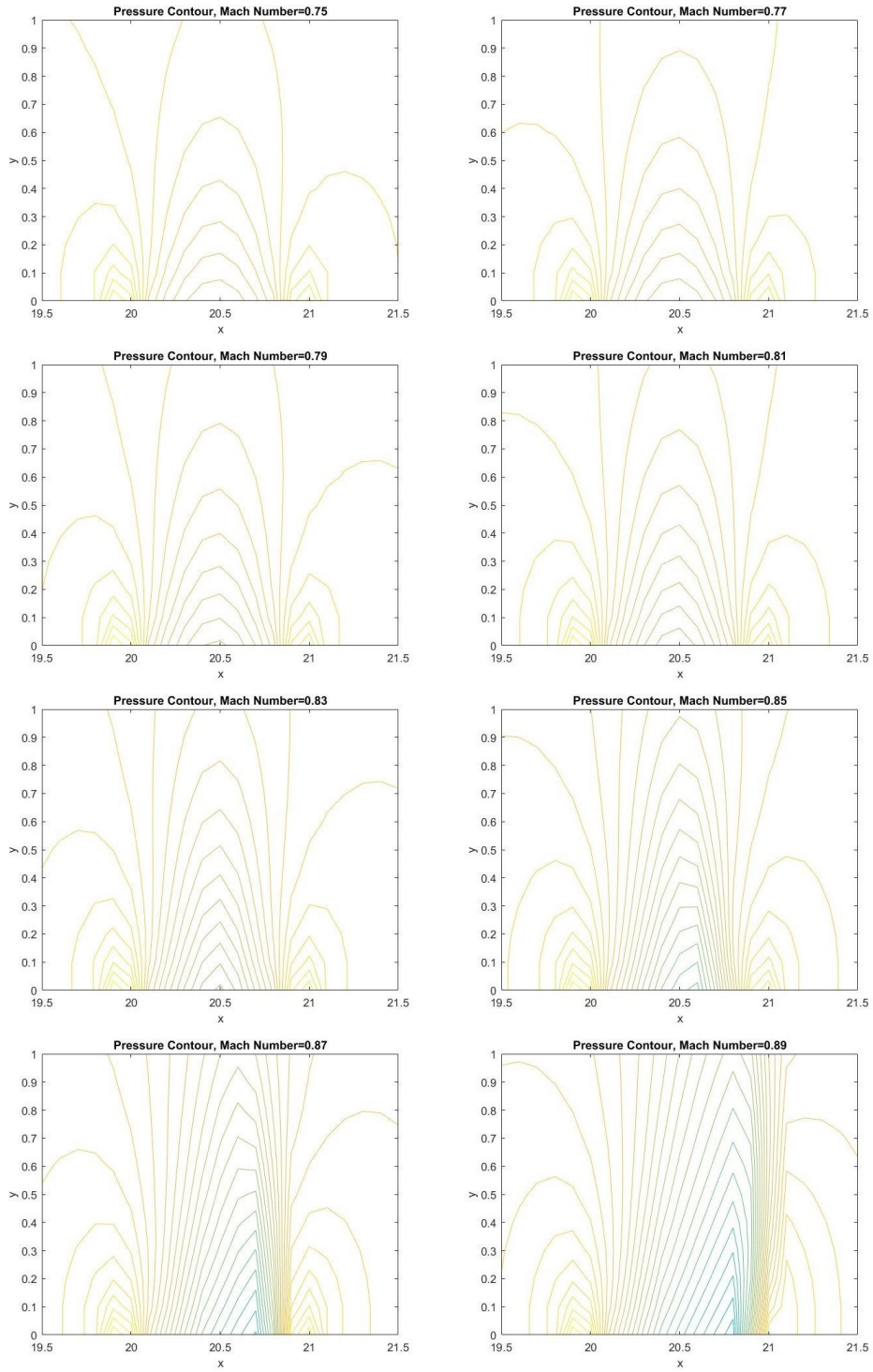

Figure 4: Pressure contours, coarse grid, various Mach Numbers.

Question 3

To study the effect of increasing grid density on the results, three different grid sizes were used. For the coarse grid, 501 points (including endpoints) were taken in x and y direction from 0 to 50, giving an increment of 0.1. For the medium grid, 1001 points were taken in x and y direction from 0 to 50, giving an increment of 0.05. For the fine grid, 2001 points were taken in x and y direction from 0 to 50, giving an increment of 0.025. The leading edge of airfoil is located at x = 20 and trailing edge is located at x = 21.

The plot of pressure coefficient over surface of the airfoil at Mach 0.80 is shown in Figure 5, where no obvious shock can be observed. All three grid plots show a trend with c_p decreasing gradually from $x = 20$ to its minimum value around $x = 20.5$, and then increasing sharply from around $x = 20.5$ to $x = 21$.

Since no shock was be observed at Mach 0.80, not much can be said about the shock location. Therefore, to obtain a better understanding about shock locations, the same pressure coefficient plot with the three grid sizes was done for Mach 0.85, as shown in Figure 6. A shock can be observed for all three grid sizes. As the grid sizes gets finer, it appears that the shock location moves slightly downstream, and that the shock gets "sharper" (a more rapid increase in pressure). All three computations predict similar shock wave location. The slight change in shock location might simply be due to the fact that the coarse grid does not have enough points to accurately describe the curve for pressure recovery, where the pressure increases sharply from its minimum value to the value at the trailing edge. For the coarse grid, there are only 10 points on the airfoil surface, whereas for the fine grid, a total of 40 points were used to describe the pressure coefficient along airfoil from 20 to 21. In this case, the low resolution caused by the shortage of points on the airfoil is the main cause of what seems to be a shock location change.

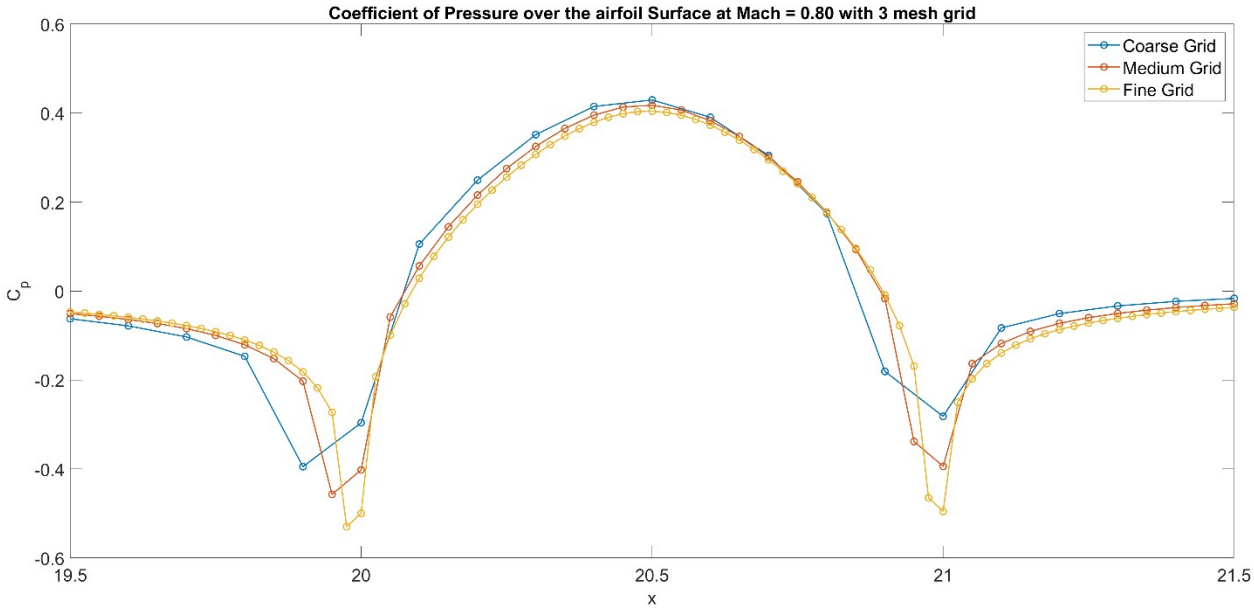

Figure 5: Coefficient of pressure (with negative pointing upwards) over the airfoil surface at Mach 0.80, calculated using three different grid sizes.

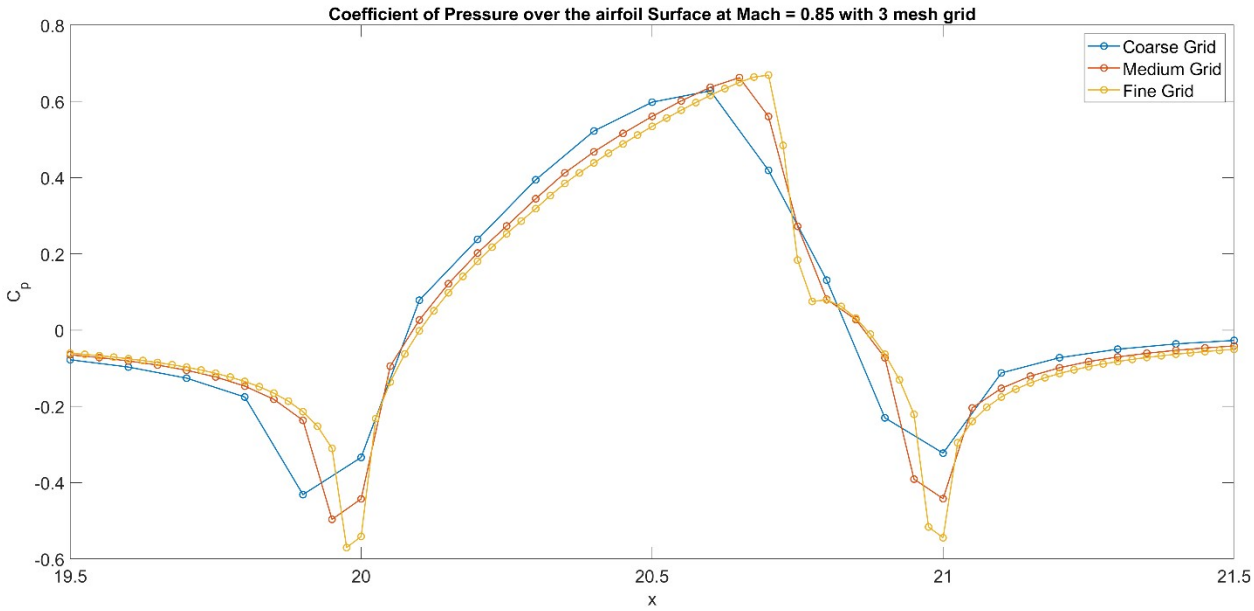

Figure 6: Coefficient of pressure (with negative pointing upwards) over the airfoil surface at Mach 0.85, calculated using three different grid sizes.

Question 4

To study the effect of freestream Mach numbers on the pressure along the airfoil, we ran the simulation for Mach numbers between 0.75 and 0.85 with 0.02 increments and compared the corresponding coefficient of pressure plots. To see the changes more clearly, we decided to use the fine grid which has a spacing of 0.025. It took between 8000 to 14000 iterations for the algorithm to converge for each Mach number. The algorithm converges slower for higher Mach number as supersonic regions kick in and the resulting velocity potential becomes more complex in certain areas. Figure **??** illustrates the effect of increasing Mach number from 0.75 to 0.85 on the pressure along the airfoil. Note that the graph is inverted, such that a value greater than zero indicates a pressure lower than the freestream pressure, while a value smaller than zero indicates a pressure higher than the freestream pressure.

For the first four freestream Mach numbers (0.75, 0.77, 0.79 and 0.81), the coefficient of pressure plot is highly symmetric, indicating that the flow does not reach Mach 1.0 on the airfoil at these relatively low freestream velocities, and that shock waves are not present. On the other hand, shock formations are clear for the two highest Mach numbers that we investigated (0.83 and 0.85). At Mach 0.83, a small shock forms at about 60% of the airfoil chord from the leading edge. At the shock location, pressure increases rapidly over a small distance, before the rate of pressure change restores to the normal rate (as at lower Mach numbers), indicating the end of the shock. At Mach 0.85, the shock is much more significant. At about 70% of the airfoil chord from the leading edge, pressure starts to increase extremely rapidly over a very short distance, before suddenly holding constant for a short distance and beginning to increase at a normal rate. As Mach number increases, it appears that the shock becomes stronger but occurs later on the airfoil. At Mach 0.85, as compared to Mach 0.83, the shock occurs much later while the pressure change during the shock is significantly larger. Additionally, the shock appears to be "sharper" at higher Mach numbers, as indicated by the sharper edges of the coefficient of

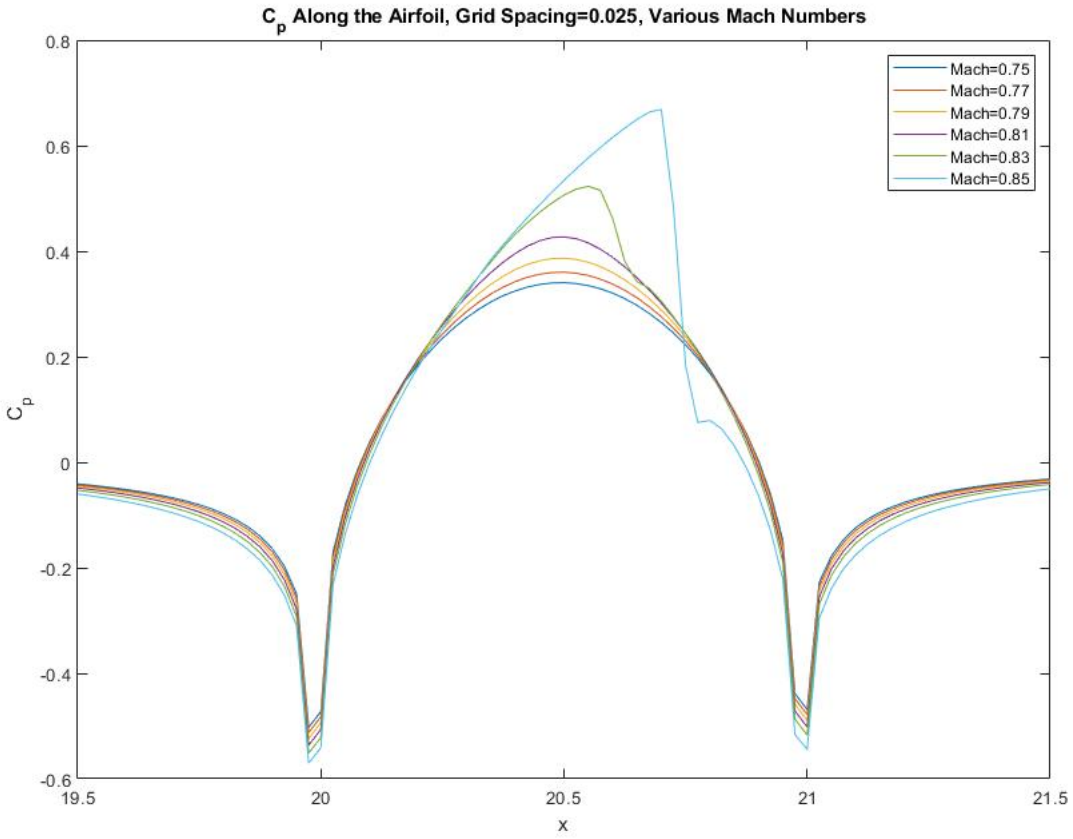

Figure 7: Coefficient of pressure along the airfoil, fine grid, at various Mach numbers

pressure plot at the beginning of the shock. However, since we only have two data points with shock formation, we could not draw any definitive conclusion regarding the effect of increasing Mach number on shock formation. More Mach numbers, including ones higher than 0.85, need to be examined in terms of shock strength and shock location.

Error Analysis

Since the TSD equation is solved numerically based on finite-difference approximations by discretizing the domain on which the solution is defined. The truncation error and round-off error where the method introduces must be considered. Truncation error is introduced by utilizing central difference and backward difference formula to discretize TSD equation. The central difference formula is used for points within the bottom boundary conditions, and it has a second order accuracy. The backward difference formula has a first order accuracy and is used on the boundary condition between leading edge and trailing edge. This indicates that the truncation error caused by backward difference is larger than central difference. To reduce the truncation error, one can use a smaller step size value of h, in other words, make the grid mesh finer. The round-off error involved in this method would be relatively small since the step value h used is relatively large ranging from 0.1 to 0.025, and MATLAB uses a machine precision of 10^{-16}. This means that the subtraction cancellation error term $\frac{\varepsilon}{h}$ is negligible in comparison to truncation error. In addition, subtraction cancellation error will not become significant until h gets unnecessarily small.

Conclusion

In this project, a simplified Murman Cole scheme is used to investigate steady transonic flow past a circular-arc shape airfoil. The governing non-linear partial differential equation contains features of mixed subsonic and supersonic flow with embedded shock waves. Finite difference formulas are developed to discrete the TSD equation. By implementing proper boundary conditions, the equations were then solved by point Gauss-Seidel method which converges well. It can be found that it generally takes iterations in the order of 10^4 to reach a residual error of less than 10^{-4} for all grid sizes. By increasing the Mach number, a shock starts to appear on the downstream side of the airfoil at Mach numbers greater than or equal to 0.83. The location of the shock remains fairly close for results obtained from all three grid sizes under the same Mach number condition. However, the location can be more accurately described using fine grid mesh as it provides a smaller truncation error than coarse grid. Furthermore, by plotting coefficient of pressure over the airfoil at various Mach number on the same graph, we found that as Mach number increases, the shock becomes stronger but occurs closer to the trailing edge.

For future work, we can further investigate TSD in the following four ways:

1. Higher Mach number can be used to solve the TSD equation for further studying the effect of shock since we currently only have two obvious shock locations at Mach 0.83 and 0.85. In addition, investigate more Mach numbers with smaller increments (0.2 in this project).

2. A finer mesh grid can be used to obtain more accurate results since it would introduce smaller truncation error.

3. Other more sophisticated fixed-point methods, such as successive over-relaxation, can be used to optimize CPU time and residual error, so that finer grids can be used.

4. A simplified governing equation is used in this project. To achieve higher accuracy, a more sophisticated equation should be used.

Bibliography

[1] J. D. Cole E. M. Murman. "Calculation of Plane Steady Transonic Flows." In: *AIAA Journal* 9.1 (1971), pp. 114–121. DOI: https://doi.org/10.2514/3.6131.

[2] S. Nadarajah. *Murman and Cole Method for Transonic Small Disturbance Equation*. URL: https://mycourses2.mcgill.ca. (accessed: 04.12.2019).